Plant Physiol. (1991) 97, 943–953
0032-0889/91/97/0943/11/$01.00/0

Received for publication April 24, 1991
Accepted July 13, 1991

High Affinity Transport of CO_2 in the Cyanobacterium *Synechococcus* UTEX 625[1]

George S. Espie[2]*, Anthony G. Miller, and David T. Canvin

Department of Biology, Concordia University, Montreal, Quebec, Canada H3G 1M8 (G.S.E.); Department of Biology, St. Francis Xavier University, Antigonish, Nova Scotia, Canada B2G 1C0 (A.G.M.); and Department of Biology, Queen's University Kingston, Ontario, Canada K7L 3N6 (D.T.C.)

ABSTRACT

The active transport of CO_2 in *Synechococcus* UTEX 625 was measured by mass spectrometry under conditions that preclude HCO_3^- transport. The substrate concentration required to give one half the maximum rate for whole cell CO_2 transport was determined to be 0.4 ± 0.2 micromolar (mean ± standard deviation; $n = 7$) with a range between 0.2 and 0.66 micromolar. The maximum rates of CO_2 transport ranged between 400 and 735 micromoles per milligram of chlorophyll per hour with an average rate of 522 for seven experiments. This rate of transport was about three times greater than the dissolved inorganic carbon saturated rate of photosynthetic O_2 evolution observed under these conditions. The initial rate of chlorophyll *a* fluorescence quenching was highly correlated with the initial rate of CO_2 transport (correlation coefficient = 0.98) and could be used as an indirect method to detect CO_2 transport and calculate the substrate concentration required to give one half the maximum rate of transport. Little, if any, inhibition of CO_2 transport was caused by HCO_3^- or by Na^+-dependent HCO_3^- transport. However, $^{12}CO_2$ readily interfered with $^{13}CO_2$ transport. CO_2 transport and Na^+-dependent HCO_3^- transport are separate, independent processes and the high affinity CO_2 transporter is not only responsible for the initial transport of CO_2 into the cell but also for scavenging any CO_2 that may leak from the cell during ongoing photosynthesis.

The efficient assimilation of CO_2 by cyanobacteria during photosynthesis depends upon the concurrent operation of a mechanism to concentrate CO_2 at the site of carboxylation (15, 28). Unlike photosynthetic cells of higher plants which rely primarily on CO_2 diffusion (9), cyanobacteria acquire DIC[3] from their environment through the active transport of CO_2 and HCO_3^- (3, 6, 18, 23). These transport processes lead to the accumulation and maintenance of a large intracellular pool of DIC from which CO_2 is fixed by Rubisco (15, 28). In cells in which the CO_2-concentrating mechanism is highly induced, intracellular [DIC] in excess of 1000 times the extracellular [DIC] has been observed (6, 15).

The mechanism by which DIC permeates cyanobacterial cells has been the subject of recent discussions (3, 23, 27). It now appears that both CO_2 and HCO_3^- serve as substrates for a DIC transport system (1, 3, 13, 14, 18, 22, 31). Transport is light dependent, requires Na^+, and is blocked by inhibitors of energy metabolism such as DCMU, carbonyl cyanide *m*-chlorophenylhydrazone, and diethylstilbestrol (13, 18, 21, 23, 28). During steady-state photosynthesis, uptake of both DIC species occurs simultaneously against their electrochemical potentials (3, 12, 23). The ability of cyanobacteria to transport and accumulate DIC is, however, greatly influenced by the DIC concentration experienced during growth. Cells grown at high [DIC] (*e.g.* 2 mM) primarily transport CO_2 (2, 7, 19), have a low apparent photosynthetic affinity for DIC ($K_{½}$ 200 μM at pH 8.0), and accumulate DIC to approximately 10- to 50-fold that present in the surroundings. Growth at low [DIC] (<500 μM) induces an ability to transport HCO_3^- (1, 6, 18), a high apparent photosynthetic affinity for DIC ($K_{½}$ 3–5 μM), and a large DIC accumulation ratio.

Several mechanisms for DIC transport have been proposed to account for these observations (3, 14, 25, 27). In low DIC-grown cells of *Synechococcus* PCC 7942 (3, 25) a "front-end" mechanism with vectorial, CA-like properties is thought to convert extracellular HCO_3^- to CO_2 for use by a CO_2-utilizing transporter. The transporter itself converts this CO_2 back to HCO_3^- during passage across the membrane so that as originally proposed in *Anabaena* (31) it is HCO_3^- that is released inside the cell. The CO_2 transporter also uses CO_2 directly from the medium. This may be the transport unit that is retained when cells are grown in high levels of DIC, whereas loss of HCO_3^- transport activity results from loss of the front end. In *Anabaena variabilis* (31), it has been suggested that CO_2 transport activity may be due to a front-end mechanism that converts extracellular CO_2 to HCO_3^- for use by a HCO_3^--utilizing pump. This pump also uses HCO_3^- directly from the medium. Conceivably, loss of the pump's ability to directly utilize HCO_3^- may account for the loss of HCO_3^- transport activity in high DIC-grown cells.

With *Synechococcus* UTEX 625, we have recently found that carbonyl sulfide (22) and H_2S (14) inhibit CO_2 transport without greatly affecting Na^+-dependent HCO_3^- transport, and monensin, Li^+, and the lack of millimolar concentrations of Na^+ inhibit HCO_3^- transport much more effectively than CO_2 transport (13, 21). Because CO_2 and Na^+-dependent

[1] Supported by grants from the Natural Sciences and Engineering Research Council of Canada.

[2] Present address: Department of Botany, Erindale College, University of Toronto, Mississauga, Ontario, Canada L5L 1C6.

[3] Abbreviations: DIC, dissolved inorganic carbon (CO_2 + HCO_3^- + CO_3^{2-}); BTP, 1,3-bis(tris[hydroxymethyl]methylamino)-propane; CA, carbonic anhydrase; EZA, ethoxyzolamide; $K_{½}$, substrate concentration required to give one-half the maximum rate.

HCO_3^- transport can be separated into discrete events in this cyanobacterium, we have proposed that two distinct paths for DIC entry into the cell exist (14). One is constitutive and utilizes CO_2 from the medium, whereas the other is inducible and utilizes HCO_3^- from the medium. The possibility of front-end mechanisms associated with the two paths of DIC entry in this cyanobacterium remains to be evaluated, as does Na^+-independent HCO_3^- (10).

To understand further the nature of the CO_2 transport process and its relationship to HCO_3^- transport, we established in this study conditions necessary for the preferential uptake of CO_2 into cells that are capable of both CO_2 and HCO_3^- transport. We also examined the effects of $[HCO_3^-]$ on CO_2 transport and analyzed the kinetics of CO_2 transport, separate from that of HCO_3^- transport. As shown by MS, the affinity of the transport system for CO_2 is much higher than previously thought, and there is sufficient capacity to support maximum rates of photosynthesis even in the absence of HCO_3^- transport. Bicarbonate proved to be an extremely weak inhibitor of CO_2 transport, although $^{12}CO_2$ effectively inhibited $^{13}CO_2$ uptake. Transport of CO_2 was also accompanied by substantial quenching of Chl *a* fluorescence. A strong, positive correlation between the initial rate of fluorescence quenching and the initial rate of CO_2 transport was found. It is concluded that fluorescence measurements provide a convenient, noninvasive means of following the kinetics of the formation of the internal inorganic carbon pool.

MATERIALS AND METHODS

Organism and Growth

The unicellular cyanobacterium *Synechococcus* UTEX 625 (*S. leopoliensis*, University of Texas Culture Collection, Austin, TX) was grown with air bubbling (0.05%, v/v, CO_2) in a modified, unbuffered Allen's medium at 30°C as described previously (10, 13). Cells were harvested at a [Chl] of 6 to 9 $\mu g \cdot mL^{-1}$ at which time the culture pH was between 9.5 and 10.2. The [DIC] in the growth medium at harvest time was between 25 and 100 μM. Cells grown in this manner generally possess the Na^+-dependent mechanism for HCO_3^- transport with little Na^+-independent HCO_3^- transport capability (10). However, we routinely tested all batch cultures to ensure that this was the case.

Experimental Conditions

Cells were washed three times by centrifugation (1 min at 10,000*g*, Beckman Microfuge B) and resuspended (7.5 to 9.5 μg Chl mL^{-1}) in 25 mM BTP/23.5 mM HCl buffer, pH 8.0, which was essentially free of DIC (15 μM) and Na^+ (5 μM). Washed cells (6 mL) were subsequently placed in a thermostatted (30°C) glass reaction vessel (20 mm diameter) and purged with N_2 to reduce the $[O_2]$ to <75 μM. The chamber was then closed to the atmosphere and the cells were allowed to temperature equilibrate for several minutes in darkness. The cell suspension was continuously stirred with a magnetic stirrer. Actinic light was provided by a tungsten-halogen projector lamp with 210 $\mu mol \cdot m^{-2} \cdot s^{-1}$ PPFD incident upon the front surface of the cuvette. The [Chl] of cell suspensions was determined spectrophotometrically at 665 nm after extraction in methanol (10) and ranged between 7.5 and 9.5 $\mu g \cdot mL^{-1}$.

Aqueous solutions of CO_2 were prepared by continuously bubbling acidified (2 mM HCl) ice-cold distilled H_2O with 5%, v/v, CO_2. The concentration of the stock CO_2 was measured with MS as described previously (14) and found to be between 3.6 and 3.9 mM.

MS

The concentration of dissolved $^{12}CO_2$ (m/e = 44), $^{13}CO_2$ (m/e = 45), and O_2 (m/e = 32) in cell suspensions was determined with a magnetic sector mass spectrometer (VG Gas Analysis, Middlewich, England; model MM 14–80 SC) equipped with a membrane-covered inlet system. The inlet tube was inserted into a port in the reaction vessel which permitted continuous measurement of dissolved gas concentrations (12, 20). The output signal from the mass spectrometer was directed to a chart recorder (14). Calibration for CO_2 and O_2 was performed as described previously (12, 20). The mass spectrometer measures dissolved CO_2, not HCO_3^- or CO_3^{2-} because these ions cannot cross the dimethyl silicone inlet membrane.

CO_2 Transport

Cells were assayed for CO_2 transport activity as described previously (14).

Chl *a* Fluorescence Yield

Changes in Chl *a* fluorescence yield, which occurred as a result of CO_2 and/or HCO_3^- transport (21, 24), were measured with a pulse amplitude modulation fluorometer (PAM-101, H. Walz, D-8521, Effeltrich, FRG). Actinic light to drive photosynthesis and DIC transport was provided at a photon flux of 210 $\mu mol \cdot m^{-2} \cdot s^{-1}$, and fluorescence yield was monitored by a weak pulse modulated beam (approximately 2 $\mu mol \cdot m^{-2} \cdot s^{-1}$ PPFD at 100 KHz) provided simultaneously by a light-emitting diode. For illuminated *Synechococcus* UTEX 625 cells, near-maximum fluorescence yield (F_m^*) was achieved in the complete absence of DIC following a brief (1 s) flash of high intensity (1600 $\mu mol \cdot m^{-2} \cdot s^{-1}$ PPFD) white light. Changes in fluorescence yield are expressed as a percentage of the variable fluorescence (F_v), where $F_v = F_m^* - F_0$. The F_0 was determined with dark-adapted cells as the fluorescence that occurred during illumination of cells with the weak modulated beam alone. The fluorescence yield and the flux of CO_2 or O_2 were measured simultaneously by placing one end of the fiber optic system of the fluorometer at the surface of the mass spectrometer reaction cuvette.

RESULTS

The ability of cyanobacteria to transport CO_2 can be determined by providing cells with a "pulse" of CO_2 and following its disappearance from the medium with MS (Fig. 1). In darkened cell suspensions or in buffer alone, the $[CO_2]$ in the reaction vessel rapidly increased to a maximum level within a few seconds of CO_2 addition and then decreased to near the initial level as the CO_2 was converted nonenzymatically to

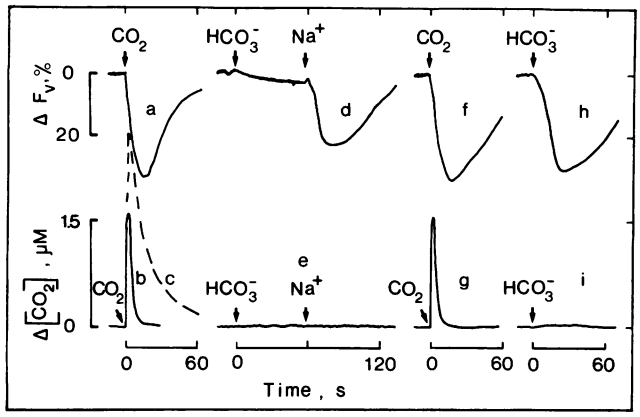

Figure 1. Simultaneous measurements of the effect of CO_2 or HCO^-_3 (10 μM) additions on Chl *a* fluorescence yield (a, d, f, and h) and extracellular $[CO_2]$ (b, c, e, g, and i) in illuminated *Synechococcus* cells (210 $\mu mol \cdot m^{-2} \cdot s^{-1}$, 9.2 μg Chl $a \cdot mL^{-1}$) at the CO_2 compensation point, either in the absence or presence of 25 mM NaCl. Arrow, Time of each addition. Before additions, fluorescence yield was near the maximum level. CO_2 was added to the cell suspension as a small volume of acidified water (2 mM HCl) saturated at 0°C with 5% CO_2. Dashed curve (c), change in $[CO_2]$ following its addition to cells in the dark. Bicarbonate was added from a stock of K_2CO_3. Assays were performed at 30°C in BTP/HCl buffer, pH 8.0, containing 100 μM NaCl.

HCO_3^- (Fig. 1c). At pH 8, only 1.6% of the added CO_2 would remain as such at equilibrium (8). With illuminated cells at the CO_2 compensation point (Fig. 1b), the increase in $[CO_2]$ following the CO_2 pulse was much smaller, and the $[CO_2]$ decreased to near zero much more rapidly than in the dark control, indicating a light-dependent uptake of CO_2. Immediately, when CO_2 was added, a large and rapid decrease in Chl *a* fluorescence yield also occurred (Fig. 1a). In previous work (21), we have shown that the extent of this fluorescence quenching is directly correlated to the magnitude of the intracellular DIC pool and is independent of C assimilation. Thus, the initial uptake of CO_2 can also be followed through fluorescence measurements when transport leads to the formation of an intracellular DIC pool (21, 24). When the DIC was assimilated, fluorescence recovered to the starting level. Initiation of the recovery phase coincided with depletion of CO_2 from the medium, but complete recovery was achieved only after the intracellular DIC pool had been consumed in photosynthesis. In this experiment, the reaction medium (Fig. 1) contained 100 μM Na^+, which is required for maximum rates of CO_2 transport (13, 19). When 10 μM HCO_3^- was added to illuminated cells under these conditions, very little change in fluorescence yield occurred, suggesting that the HCO_3^- transport system was incapable of forming a substantial intracellular DIC pool (Fig. 1d). In *Synechococcus* UTEX 625 at pH 8, high rates of HCO_3^- transport are achieved in the presence of 25 mM Na^+ (13). Addition of 25 mM NaCl to the cell suspension resulted in a substantial decrease in fluorescence (Fig. 1d). The extracellular $[CO_2]$, however, remained close to zero (Fig. 1e). With time, the fluorescence yield recovered completely and this coincided with the cessation of photosynthetic O_2 evolution (not shown). Now, in the presence of 25 mM Na^+, the addition of either CO_2 (Fig. 1f) or HCO_3^- (Fig. 1h) caused quenching of fluorescence which recovered to the initial value after the DIC was consumed in photosynthesis. In the case of HCO_3^- addition, the change in fluorescence yield was not accompanied by any change in extracellular $[CO_2]$ (Fig. 1i), whereas an obvious change in $[CO_2]$ occurred when CO_2 was added (Fig. 1g). Subsequent addition of Na^+ to the suspension in the absence of DIC did not cause any fluorescence quenching (not shown), indicating that the quenching that occurred when Na^+ was initially added (Fig. 1d) was a result of the formation of an intracellular DIC pool mediated by Na^+-dependent HCO_3^- transport (13, 18, 21, 24). Such a transport system capable of generating a large intracellular DIC pool has been previously demonstrated in several cyanobacteria (1, 3, 11, 23). Because both CO_2 and HCO_3^- additions caused fluorescence quenching (Fig. 1, f and h), it appears that at higher $[Na^+]$ both CO_2 and HCO_3^- transport occurred (13, 18, 23) but that at 100 μM Na^+ only CO_2 transport occurred.

Accurate estimates of the initial rate of CO_2 transport from CO_2-pulsing experiments (Fig. 1b) are complicated by the large decrease in $[CO_2]$ during the first 10 s of the experiment, the lack of a full response to the added CO_2, and the simultaneous hydration of CO_2. To overcome these problems, for transport studies we assessed whether or not preferential uptake of CO_2 occurred in a reaction medium containing 100 μM Na^+ and the enzyme CA, which catalyzes the equilibration of CO_2 and HCO_3^-.

In the past, we have assumed that the increase in the magnitude of the intracellular DIC pool and rate of photosynthesis that occurred when CA was added to cell suspensions was a consequence of increased CO_2 transport, which was facilitated by CA maintaining the $[CO_2]$ in the medium at equilibrium with $[HCO_3^-]$ (18). This view is supported by the results shown in Figure 2. In this experiment, cells were provided with 50 to 60 μM DIC. During illumination, the cells caused the $[CO_2]$ to decrease to near zero, although a considerable amount of HCO_3^- remained in the medium, out of chemical equilibrium with CO_2. Addition of CA to the suspension resulted in an increase in $[CO_2]$ which increased through the CA-mediated dehydration of HCO_3^- (Fig. 2B). At the same time, a corresponding decrease in fluorescence yield occurred, signifying the formation of an intracellular DIC pool (Fig. 2A). Because the $[HCO_3^-]$ declined (1.6%) by the same amount as the $[CO_2]$ increased when CA was added, it seems likely that pool formation was mediated by CO_2 rather than HCO_3^- transport, particularly because $[Na^+]$ was far below the optimum for HCO_3^- uptake. Following the initial decline, a new steady-state level of fluorescence was established which reflected the quenching due to carbon fixation and the steady-state intracellular [DIC] (Fig. 2A). Ultimately, fluorescence returned to its initial level as the CO_2 was consumed, and this coincided with the depletion of CO_2 (DIC) from the medium (Fig. 2, A and B).

It is possible that CA (Fig. 2) in some way mimicked the effect of Na^+ on HCO_3^- transport and that the intracellular DIC pool was, in fact, formed by this transport system instead. Figure 2, C and D, however, shows that it is the catalytic activity of CA, rather than some other property, that is necessary to elicit the decrease in Chl *a* fluorescence yield

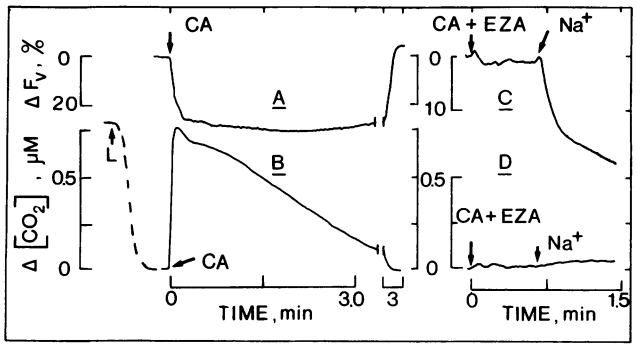

Figure 2. The effect of CA, CA + EZA, and Na^+ on Chl *a* fluorescence yield and extracellular $[CO_2]$. Cell suspensions containing 50 to 60 μM DIC were illuminated (L↑; 210 $\mu mol \cdot m^{-2} \cdot s^{-1}$) and allowed to selectively deplete the medium of CO_2 (B, dashed line). At this point, 25 $\mu g \cdot mL^{-1}$ CA was added and changes in Chl *a* fluorescence yield (A) and extracellular $[CO_2]$ (B) were simultaneously recorded by the PAM-101 fluorometer and MS. In a similar experiment, fluorescence yield (C) and extracellular $[CO_2]$ (D) were measured simultaneously following the addition of CA previously incubated with 50 μM EZA. NaCl was subsequently added to give a final concentration of 25 mM. The CO_2 depletion phase is not shown in D. Note the different scales for fluorescence. Cell suspensions originally contained 100 μM NaCl and 9.0 (A and B) or 8.3 (C and D) μg Chl $a \cdot mL^{-1}$.

(Fig. 2A). Initial conditions were established as before. Then the cells were provided with CA previously incubated with EZA. EZA is a potent inhibitor of CA which binds to the catalytically essential Zn within the active site. Addition of inhibited CA caused no increase in CO_2 concentration and only a small change in fluorescence yield (Fig. 2, C and D). The ability of cells to transport HCO_3^- in the presence of CA + EZA appeared to be normal because the addition of 25 mM Na^+ elicited a large change in fluorescence yield without an increase in extracellular $[CO_2]$ (Fig. 2, C and D). The presence of low levels of EZA (20–50 μM) alone had no significant effect on CO_2 or Na^+-dependent HCO_3^- transport (data not shown), which is in agreement with previous findings for *Synechococcus* PCC 7942 (5, 26). Collectively, the data indicate that, in the presence of CA and 100 μM Na^+, HCO_3^- transport does not occur and CO_2 transport is the predominant means of organic carbon uptake by *Synechococcus* cells at pH 8.

Kinetics of CO_2 Transport

The transport of CO_2 was measured either as CO_2 disappearance from the medium or, indirectly, by monitoring the formation of the intracellular DIC pool using fluorescence quenching as an indicator (Fig. 3). Transport was initiated by the addition of K_2CO_3 to illuminated cell suspensions containing 25 $\mu g \cdot mL^{-1}$ CA and 100 μM Na^+. Because equilibrium between CO_2 and HCO_3^- was maintained by CA, the instantaneous $[CO_2]$ for kinetic experiments was calculated as 1.6% of the DIC added. Under these conditions, it was found that the $[CO_2]$ increased to the expected level and then remained constant when DIC was added to darkened cells (Fig. 3A). With illuminated cells the $[CO_2]$ did not reach the same level as with darkened cells, and a few seconds after DIC addition a rapid decline in $[CO_2]$ occurred (Fig. 3A). The decline during the first 15 s was taken as the initial rate of CO_2 transport. The change in $[CO_2]$ during this period, however, was much less than that which occurred in the absence of CA (compare Figs. 1 and 3). Because of the response time (2–3 s) of the mass spectrometer and the cell densities used, a full response to the DIC added to illuminated cells was not observed. Extrapolation of the initial uptake curve back to time zero yielded a $[CO_2]$ close to that expected from the dark control, indicating that CO_2 transport did not occur at a significantly faster rate during the unresolved time (5 s) than that used (5–15 s) to estimate the initial rate.

The disappearance of CO_2 from the medium involves contributions from both transport and CO_2 fixation. Fixation during the initial phase of CO_2 disappearance, however, was only a very minor component of the total (Fig. 3C). As judged by fluorescence quenching, the intracellular DIC pool was at a maximum value 24 s after DIC addition (Fig. 3B). At this time, about 65% of the CO_2 (DIC) had been removed from the medium, but, as indicated by O_2 evolution, <10% had been fixed. Even less fixation would have occurred during the first 15 s. That photosynthesis was in fact a minor component

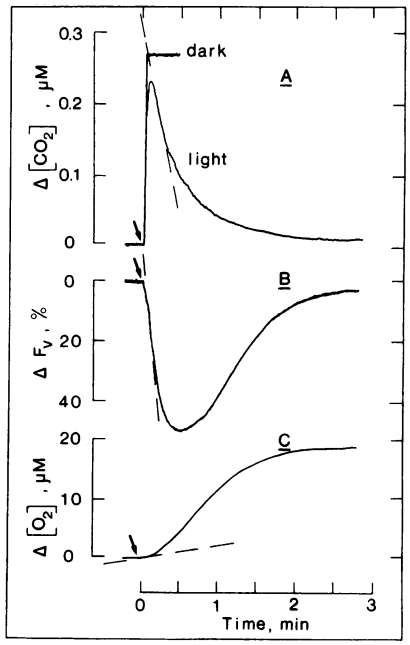

Figure 3. Simultaneous measurements of the initial rate of CO_2 transport (A) and fluorescence quenching (B) along with parallel measurements of photosynthetic O_2 evolution (C). *Synechococcus* cells (9.5 μg Chl $a \cdot mL^{-1}$) were suspended in 25 mM BTP/HCl buffer, pH 8.0, containing 100 μM NaCl and 25 $\mu g \cdot mL^{-1}$ CA. Illuminated (210 $\mu mol \cdot m^{-2} \cdot s^{-1}$) cells were allowed to go to the CO_2 compensation point as indicated by the cessation of O_2 evolution or the return of Chl *a* fluorescence to near-maximum yield. In this example, CO_2 transport was initiated by the addition of 17 μM DIC (arrows). A, Changes in $[CO_2]$ measured with MS at m/e = 44 in the light and dark (as indicated). Dashed line, Initial rate of CO_2 transport, fluorescence quenching, or O_2 evolution was determined during the first 15 s of the time course. The response time of MS to CO_2 and O_2 was 2 to 3 s.

in the initial disappearance of CO_2 was verified with cells in which the Calvin cycle was inhibited by iodoacetamide (Fig. 4). In inhibited and noninhibited cells, the initial rate of CO_2 uptake was similar, as was the initial change in fluorescence yield. During darkening, the CO_2 removed from the medium by iodoacetamide-poisoned cells was released back into the medium, demonstrating that only transport, but not fixation, had occurred.

The rate of CO_2 transport as a function of extracellular $[CO_2]$ is shown in Figure 5. These measurements were made without iodoacetamide present in the medium because the initial rates of CO_2 transport were usually >100-fold greater than the initial rate (at 15 s) of photosynthetic O_2 evolution (Fig. 5). The CO_2 uptake curve showed saturation characteristics, and maximum rates were obtained between 1.0 and 1.5 μM CO_2. In seven different experiments, the maximum rate of transport was between 400 and 735 μmol $CO_2 \cdot mg^{-1}$ Chl $\cdot h^{-1}$ and averaged 522 μmol $CO_2 \cdot mg^{-1}$ Chl $\cdot h^{-1}$. This rate was about three times greater than the DIC-saturated rate of photosynthetic O_2 evolution typically observed under these conditions. In five of seven cases, the maximum rate of transport predicted from Lineweaver-Burke plots was within 10% of the observed value and deviated by <60% in the remaining cases. The $K_{1/2}$ for CO_2 transport was estimated to be 0.4 ± 0.2 μM (mean ± SD; n = 7) and was found to range between 0.2 and 0.66 μM (*e.g.* Fig. 5, inset).

When the initial rate of fluorescence quenching, as a percentage of the maximum rate, is normalized to the maximum rate of CO_2 transport and plotted as a function of $[CO_2]$ (Fig. 5), it can be seen that the kinetics of fluorescence quenching tracks that of CO_2 transport. This relationship holds only

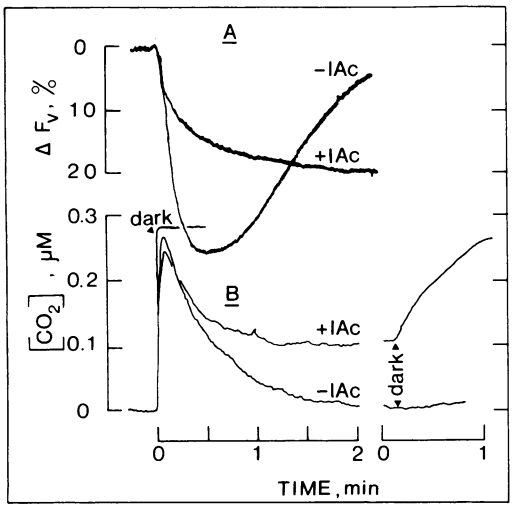

Figure 4. Effect of photosynthetic carbon fixation on Chl *a* fluorescence quenching (A) and CO_2 transport (B). The assay was initiated by adding 17 μM DIC to an illuminated (210 μmol $\cdot m^{-2} \cdot s^{-1}$, 8.5 μg Chl *a* $\cdot mL^{-1}$) cell suspension containing 100 μM NaCl and 25 $\mu g \cdot mL^{-1}$ CA, in the absence or presence of 3.3 mM iodoacetamide (IAc) to inhibit carbon fixation (20). Iodoacetamide-poisoned cells were subsequently placed in darkness (B), and reappearance of CO_2 in the medium was monitored. B, increase in $[CO_2]$ following addition of 17 μM DIC to darkened cells.

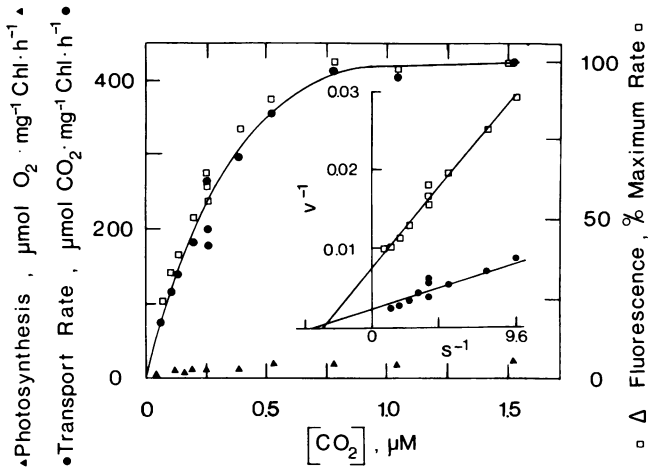

Figure 5. The initial rate of CO_2 transport (●), photosynthesis (▲), and fluorescence quenching (□) as a function of $[CO_2]$. The initial rates were determined in the presence of 100 μM NaCl and 25 $\mu g \cdot mL^{-1}$ CA from the first 15 s of time-course experiments as described in Figure 3. The data are from one of seven experiments. Fluorescence quenching data are plotted as a percentage of the maximum rate of fluorescence quenching. The 100% value was set to correspond to the maximum rate of CO_2 transport. Inset, Double reciprocal plot of rate *versus* $[CO_2]$ for CO_2 transport (●) and fluorescence quenching data (□). Results are from an experiment conducted at pH 8.0, 30°C, 210 μmol $\cdot m^{-2} \cdot s^{-1}$ and 8.2 μg Chl *a* $\cdot mL^{-1}$.

during the initial phase of CO_2 uptake and is likely due to a close coupling between CO_2 transport and pool formation, which then elicits a change in fluorescence yield rather than to any direct relationship between transport rate and fluorescence quenching (21). The transient nature of the relationship is also evident in the experimental results shown in Figure 3, where after the initial decline in fluorescence the yield began to increase even though CO_2 transport continued. Nevertheless, because pool filling resulted in fluorescence quenching and was mediated solely by CO_2 transport, under our conditions, fluorescence measurements provide a convenient alternate means of estimating the $K_{1/2}$ for CO_2 transport (Fig. 5, inset). Based on this approach, a $K_{1/2}$ of 0.25 ± 0.1 μM (mean ± SD; n = 7) was calculated. Because the initial rate was measured as a change in fluorescence in this case, a value for V_{max} in units of μmol $CO_2 \cdot mg^{-1}$ Chl $\cdot h^{-1}$ could not be calculated.

Accurate estimates of CO_2 efflux from the cells during the initial phase of pool formation are difficult to make, but the reduction in the initial rate of CO_2 disappearance from the medium due to the leakage factor can be minimized if measurements are made during as short an interval as possible. Also, if, as suggested for *Anabaena variabilis* (31) and *Synechococcus* PCC 7942 (25), the transported CO_2 arrives on the inner side of the membrane as HCO_3^- or is quickly converted to HCO_3^-, the initial back flux of CO_2 will be small and our measurement of the initial rate of CO_2 transport will not significantly underestimate the actual rate.

Effect of $[HCO_3^-]$ on CO_2 Transport

The possibility of HCO_3^- inhibition of CO_2 transport (31) in *Synechococcus* cells was evaluated at various $[H^{13}CO_3^-]$

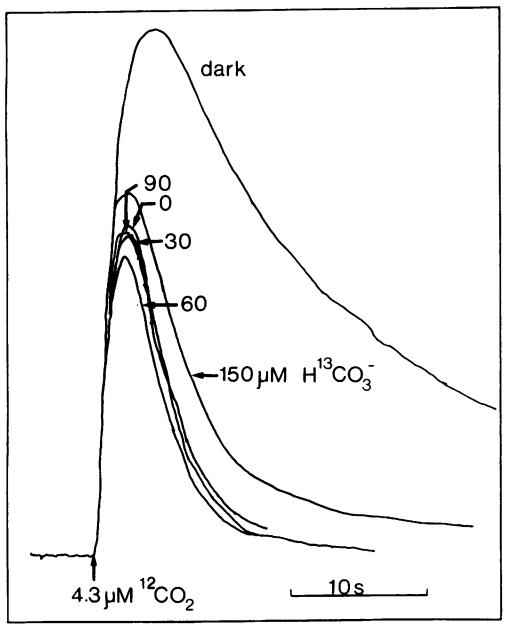

Figure 6. The effect of $[H^{13}CO_3^-]$ concentration on $^{12}CO_2$ transport. Iodoacetamide (3.3 mM) poisoned cells (8.3 μg Chl *a* mL^{-1}) at the CO_2 compensation point were provided with increasing amounts of $H^{13}CO_3^-$ in the medium, and their ability to transport CO_2 was assessed following the addition of 4.3 μM $^{12}CO_2$. Changes in $[^{12}CO_2]$ relative to the dark control were measured using an aqueous inlet mass spectrometer set at m/e = 44. Assays were performed in the presence of 25 mM NaCl to permit full HCO_3^- transport activity. CA was not added in this experiment.

using the $^{12}CO_2$-pulsing technique as an assay for CO_2 transport (Fig. 6). Advantage was taken of the fact that the cells normally deplete the medium of CO_2 at pH 8, creating a disequilibrium between CO_2 and HCO_3^- (*e.g.* Fig. 2B). Consequently, $[H^{13}CO_3^-]$ can be increased (by $DI^{13}C$ addition) without a corresponding increase in the bulk $[^{13}CO_2]$. For the cells to maintain the $[^{13}CO_2]$ near zero they must continually transport $^{13}CO_2$ at a rate equal to the uncatalyzed rate of $H^{13}CO_3^-$ dehydration. Thus, in these dual isotope experiments, $^{12}CO_2$ transport (m/e = 44) was assayed for on an increasing background of $^{13}CO_2$ uptake (m/e = 45). At 150 μM $H^{13}CO_3^-$, for example, a rate of $^{13}CO_2$ transport equivalent to 20% of V_{max} would be required to maintain $[^{13}CO_2]$ near zero. The $H^{13}CO_3^-$ was maintained at constant levels by blocking photosynthetic carbon assimilation with iodoacetamide. These procedures permit the competition experiments to be performed under steady-state conditions and provide a continuous record of CO_2 disappearance from the medium over the range of $[CO_2]$ (4.3–0 μM) experienced by the cells during a single assay. In most experiments, 25 mM Na^+ was included to maximize HCO_3^- transport and, therefore, any inhibitory effect of Na^+-dependent HCO_3^- transport may have on CO_2 transport. The range of $[H^{13}CO_3^-]$ used was sufficient to support rates of $H^{13}CO_3^-$ transport from zero to V_{max} (500 $\mu mol \cdot mg^{-1}$ Chl $\cdot h^{-1}$) and intracellular accumulation in excess of 40 mM (13, 20). Transport of HCO_3^- in the presence of iodoacetamide was indicated by Na^+-dependent fluorescence quenching (18) and by Na^+-dependent HCO_3^- accumulation measured by MS (13, 20) or the silicone fluid filtration technique (not shown).

The control level for CO_2 transport (0% inhibition) was taken as the peak height for the CO_2 uptake curve in the absence of $H^{13}CO_3^-$. The cells had previously been allowed to go to the compensation point to reduce $H^{12}CO_3^-$ to a low level as well. For most of the range of $[H^{13}CO_3^-]$ tested, no appreciable difference in CO_2 uptake was observed compared with the control (Fig. 6). Even at low $[^{12}CO_2]$ (0.1–0.5 μM) along the uptake curves, the apparent rates of CO_2 disappearance from the medium were similar over the range of $[H^{13}CO_3^-]$ tested. Progressive inhibition of CO_2 transport by increasing $[H^{13}CO_3^-]$ would be expected to result in the CO_2 uptake curves becoming more like the dark control, with extensive tailing of the curves occurring at low $[^{12}CO_2]$ and high $[H^{13}CO_3^-]$. Only at the highest $[H^{13}CO_3^-]$ tested was there evidence for some interference with CO_2 uptake (Fig. 6). A plot of a number of transport assays (n = 64) revealed a slight inhibitory effect of $H^{13}CO_3^-$ on CO_2 uptake (Fig. 7). Statistical analysis (t test) indicated that the slope of the regression line was significantly (P = 0.0007) different from zero, but the computed value of r^2 (0.11) indicated that only about 11% of the observed variability in CO_2 transport was actually explained by increasing $[H^{13}CO_3^-]$. From the regression equation, we calculated that CO_2 transport declined by about 5.9% per 100 μM $H^{13}CO_3^-$. This small effect of a large increase in HCO_3^- flux across the membrane indicates that Na^+-dependent HCO_3^- transport was either not inhibitory toward CO_2 transport or a poor inhibitior with an extremely high K_i. Uptake of CO_2 occurred in the presence and absence of 25 mM Na^+ (Fig. 1). Similar, but less extensive, results to those shown for 25 mM Na^+ have also been obtained in the presence of 100 μM Na^+ (Fig. 7) where HCO_3^- transport activity would be minimal (Fig. 1). These results suggest that the HCO_3^- ion itself does not interfere with CO_2 uptake.

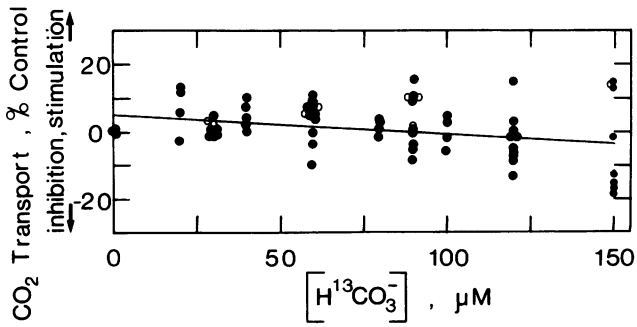

Figure 7. Summary of the effects of $[H^{13}CO_3^-]$ on $^{12}CO_2$ transport. The $[H^{13}CO_3^-]$ was varied from 0 to 150 μM, and $^{12}CO_2$ uptake was assayed as in Figure 6. The difference in the peak heights between the control and the experimental curves were plotted as a percentage of the control level of CO_2 transport ($[H^{13}CO_3^-]$ = 0 taken as 0%). Experiments were conducted in the presence of 25 mM NaCl (●) or 100 μM NaCl (○) and 3.3 mM iodoacetamide in BTP/HCl buffer, pH 8.0, and 30°C. Linear regression analysis yielded an equation of the form $y = -0.059 \times +5.2$ (r = 0.33) for the 25 mM NaCl data. The results are from seven experiments.

Inhibition of CO_2 Transport

Although $H^{13}CO_3^-$ was relatively ineffective in inhibiting $^{12}CO_2$ uptake, $^{12}CO_2$ did prove to be an effective inhibitor of $^{13}CO_2$ uptake (Fig. 8). In this experiment, iodoacetamide-poisoned cells were provided with 100 μM $K_2{}^{13}CO_3$ in the presence of 100 μM Na^+ (no HCO_3^- transport) and allowed to selectively deplete the medium of $^{13}CO_2$ as before. Subsequently, the cells were presented with pulses of varying amounts of $^{12}CO_2$, and the fate of both $^{12}CO_2$ and $^{13}CO_2$ were followed simultaneously with the MS. The addition of a pulse of $^{12}CO_2$ to buffer alone showed that the CO_2 contained only the expected natural abundance (1.1%) of $^{13}CO_2$ (Fig. 8A, curve 5). With darkened cells (1.6 μM $^{13}CO_2$ in the medium), a pulse of $^{12}CO_2$ caused only a very small increase in [$^{13}CO_2$] above that found for the buffer control (Fig. 8A, curve 4). This increase was likely due to simple exchange of intracellular $^{13}CO_2$ for $^{12}CO_2$, because CO_2 transport does not occur at an appreciable rate in the dark (20). The [$^{13}CO_2$] subsequently decreased because some of it was converted to $H^{13}CO_3^-$. With illuminated cells (about 0.1 μM $^{13}CO_2$ left in the medium), pulses of increasing amounts of $^{12}CO_2$ (Fig. 8B, curves 1–3) resulted in the transient appearance of increasing amounts of $^{13}CO_2$ in the medium. With the highest [$^{12}CO_2$] used, the [$^{13}CO_2$] increased to about one-half the level expected for $^{13}CO_2$ in equilibrium with the 100 μM $K_2{}^{13}CO_3^-$ originally added. Darkening the cells resulted in the reappearance of all of the 1.6 μM $^{13}CO_2$ expected (not shown). The increase in [$^{13}CO_2$] is most easily explained if it is assumed that $^{12}CO_2$ competed with $^{13}CO_2$ for uptake. The $^{13}CO_2$ transiently appearing in the medium could have arisen either from within the cells or from external dehydration of $H^{13}CO_3^-$. In the first case, $^{13}CO_2$ within the intracellular pool returns to the medium during the course of the normal pump-leak cycle (14, 22). In the absence of $^{12}CO_2$, the $^{13}CO_2$ leaking from the cells would be transported back into the cells by the high affinity transport system, and its concentration would remain near zero. However, because the pulse increased the initial [$^{12}CO_2$] in the medium to a level substantially higher than the [$^{13}CO_2$], $^{12}CO_2$ transport would be favored over transport of $^{13}CO_2$. Thus, the [$^{12}CO_2$] declined while the [$^{13}CO_2$] increased in the medium. Not until the medium contained similar levels of $^{12}CO_2$ and $^{13}CO_2$ did $^{13}CO_2$ begin to disappear from the medium again. This behavior is consistent with a competition between $^{12}CO_2$ and $^{13}CO_2$ for uptake.

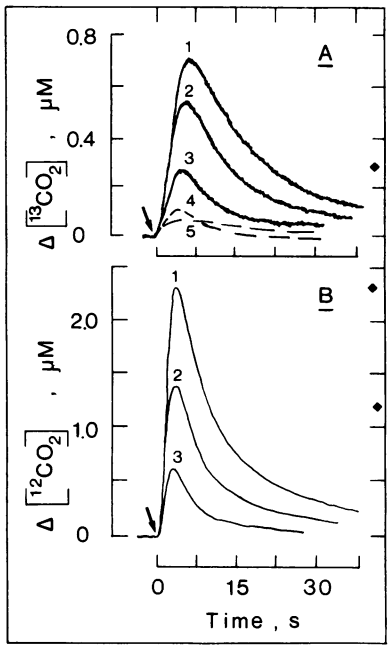

Figure 8. Effect of pulses of $^{12}CO_2$ on $^{13}CO_2$ transport by *Synechococcus* cells. Iodoacetamide (3.3 mM) poisoned cells (7.6 μg Chl *a*·mL^{-1}) at the CO_2 compensation point were provided with 100 μM $K_2{}^{13}CO_3$ in the presence of 100 μM NaCl and were allowed to selectively deplete the medium of $^{13}CO_2$ in the light (210 μmol·m^{-2}·s^{-1}) as in Figure 2B. Subsequently, the cells were presented with increasing amounts of $^{12}CO_2$ (arrows), and the fate of both $^{13}CO_2$ (A, curves 1–3; m/e = 45) and $^{12}CO_2$ (B, curves 1–3; m/e = 44) were simultaneously followed with MS. Curves having the same number in A and B are results from the same experiment (CO_2 pulse). Curves 4 and 5 (A) show the effect of $^{12}CO_2$ additions (not shown in B) on [$^{13}CO_2$] for cells in the dark or for buffer alone containing no added ^{13}C. The dark controls for curves 1 to 3 (B) are shown; ♦ represent their peak heights. Uppermost ♦ corresponds to curve 1, the middle to curve 2, and the lower to curve 3. Uppermost ♦ also represents the level of $^{12}CO_2$ provided for the experiments shown in curves 4 and 5 (A). Experiments were conducted at pH 8.0, 30°C, and CA was not added.

It is also possible that the increase in [$^{13}CO_2$] may be due to a simple one to one exchange of $^{12}CO_2$ for $^{13}CO_2$ not involving the activity of the CO_2 transport system. In this case, the intracellular [$^{13}CO_2$] would be no higher than 1.6 μM, resulting from the diffusion of $^{13}CO_2$. If all of this was exchanged from an intracellular volume of 380 μL·L^{-1} medium (58 μL·mg^{-1} Chl [13]), then the $^{13}CO_2$ transiently appearing in the medium would be no higher than 0.61 nM or 1200-fold lower than observed (Fig. 8A).

The transient appearance of $^{13}CO_2$ (Fig. 8A) could also come from $H^{13}CO_3^-$ dehydration in the medium. For the cells to maintain the [$^{13}CO_2$] near zero, as they do, it must be taken up at the same rate as it was produced from $H^{13}CO_3^-$ dehydration. Appearance of $^{13}CO_2$ in the medium meant that $^{13}CO_2$ uptake lagged behind $H^{13}CO_3^-$ dehydration. Both the intracellular pool and extracellular $H^{13}CO_3^-$ dehydration likely contributed to the increase in [$^{13}CO_2$], but regardless of the source, inhibition of $^{13}CO_2$ transport was a necessary requisite for the appearance of $^{13}CO_2$ in the medium. Furthermore, conversion of the $^{12}CO_2$ to $H^{12}CO_3^-$ was not required to inhibit $^{13}CO_2$ uptake, as was evidenced by increased $^{13}CO_2$ uptake as the $^{12}CO_2$ disappeared (Fig. 8). In the presence of ongoing HCO_3^- transport (25 mM Na^+), $^{13}CO_2$ appearance in the medium following a $^{12}CO_2$ pulse was no greater than in its absence (Fig. 9), further indicating a lack of interaction between the two mechanisms of DIC acquisition.

DISCUSSION

It is important, when determining rates of transport or the affinity of the transport system for its substrate, that only the species of inorganic carbon of interest is, in fact, transported.

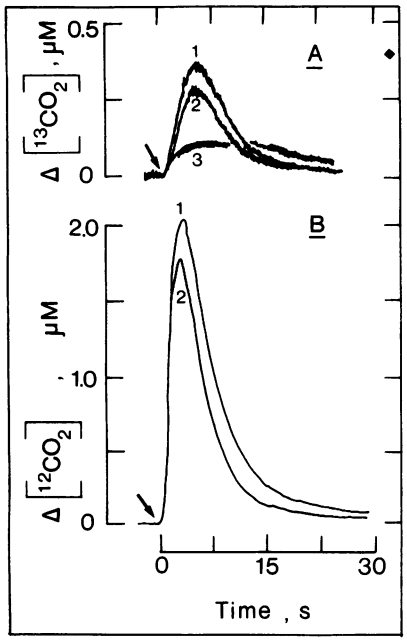

Figure 9. Effect of ongoing HCO_3^- transport on $^{12}CO_2$ and $^{13}CO_2$ transport in *Synechococcus* cells. Illuminated cells (600 μmol·m^{-2}·s^{-1}, 8.2 μg Chl *a*·mL^{-1}), in the presence of iodoacetamide (3.3 mM) and 125 μM DIC (42 μM DI^{12}C + 83 μM DI^{13}C) were allowed to selectively deplete the medium of CO_2. Pulses of $^{12}CO_2$ were subsequently provided to the cells, and the fates of $^{13}CO_2$ (A, curves 1 and 2) and $^{12}CO_2$ (B, curves 1 and 2) were simultaneously followed by MS. Curves having the same number in A and B are results from the same experiment (CO_2 pulse). Experiments were conducted in the presence of 100 μM NaCl (curve 1, A and B: no HCO_3^- transport) or 25 mM NaCl (curve 2, A and B: ongoing HCO_3^- transport). ♦, Peak height for the dark control (B, +25 mM NaCl); the corresponding effect on [$^{13}CO_2$] with cells in the dark is shown by curve 3 (A). CA was not added in this experiment.

Hence, if CO_2 is the species of interest, CO_2 transport must be measured directly and HCO_3^- transport must be absent.

It is now well established that air-grown cells of *Synechococcus* UTEX 625 can actively transport both HCO_3^- and CO_2 (10, 12, 14, 18, 22). CO_2 transport, however, only requires micromolar concentrations of Na^+ (13, 19, 20), whereas HCO_3^- transport requires millimolar concentrations (13). HCO_3^- transport then can be effectively prevented by only including a low concentration of Na^+ in the reaction medium (Fig. 1). In these circumstances the cells are confined to transporting CO_2.

The active transport of HCO_3^- or CO_2, even when fixation of CO_2 is prevented, causes the quenching of Chl *a* fluorescence (21), and the degree of quenching is highly correlated with the size of the internal pool of inorganic carbon (21, 24). Hence, quenching of fluorescence can conveniently be used as an indirect indication of transport, and it shows (Fig. 1) that in the presence of low levels of Na^+, as expected, only CO_2 is being transported.

To determine the affinity of the CO_2 transport system for its substrate, it is necessary to measure initial rates of transport as a function of the concentration of CO_2. Silicone fluid centrifugation experiments have previously been used (6, 31) to estimate the affinity of the CO_2 transport system for CO_2. With this technique, the inorganic carbon is added as CO_2 and the cells are separated from the reaction medium by spinning them through a layer of silicone fluid. Two major problems with this technique preclude the measurement of the initial rate of CO_2 transport, however. First, because of its conversion to HCO_3^- (see Fig. 1C), the CO_2 concentration quickly decreases far below the concentration that was initially added. Uptake by cells in the light greatly accelerates CO_2 disappearance to the point where after 10 s only about 10% of the initial [CO_2] remains. Second, although 5-s sampling times have been used (31), the usual first reliable sampling point is 10 s (3, 5, 20). By this time the internal inorganic carbon pool is largely filled (5, 6, 20) and, at low concentrations of CO_2, most of the CO_2 has been removed from the external medium (1, 20). Consequently, considerable uncertainty will exist as to the actual [CO_2] experienced during the transport assay.

A continuous record of the rate of transport or uptake of CO_2 can be obtained with MS, with which the 69% response time is about 3 s. Even with MS, however, initial rates of transport as a function of CO_2 concentration cannot be obtained with CO_2-pulsing experiments. (These CO_2-pulsing experiments are analogous to the addition of CO_2 in the silicone fluid centrifugation technique.) As mentioned, both the conversion of CO_2 to HCO_3^- and CO_2 uptake by the cells caused the [CO_2] to quickly decline far below the initial level within 10 s. Even in the dark, the expected [CO_2] in the reaction mixture is not observed because of the conversion of CO_2 to HCO_3^- within the resolving time of MS (Fig. 1C).

To obtain reliably the expected CO_2 concentrations in the dark, it is necessary to add CA to quickly establish the HCO_3^-/CO_2 equilibrium (Fig. 3). This, of course, completely defeats the rationale of CO_2-pulsing experiments, but the quantitative shortcomings of those experiments have already been described. There are no problems with the use of CO_2 pulsing in comparative or qualitative experiments. When CA is present in the light, the CO_2 approaches that expected (Fig. 3), and a tangent to the initial rate of CO_2 disappearance does, in fact, extrapolate through the expected zero time CO_2 concentration (Fig. 3). We thus believe that with the technique described (Fig. 3) we are able to measure the initial rates of transport of CO_2. The addition of CA also, of course, prevents the precipitous decrease of CO_2 concentration (Figs. 1, B and C, and 2B) that is observed in its absence and hence maintains the CO_2 concentration closer to the added concentration for a longer period of time.

The addition of CA did not alter the specificity of transport, because only CO_2 was still transported (Fig. 2), and hence the stimulatory affect of CA addition on internal pool filling or photosynthesis was, as assumed earlier (18), entirely due to the greater availability of CO_2 due to the maintenance of the HCO_3^-/CO_2 equilibrium.

Using the procedure and technique illustrated in Figure 3, we have determined the initial rates of transport of CO_2 by the CO_2 transport system as a function of the CO_2 concentration. It must be emphasized that the uptake of CO_2 from the medium that we measure is not due to the fixation of CO_2; it represents essentially only the transport of CO_2 from the

exterior of the cell to the interior of the cell. The initial transport of CO_2 is not greatly affected when fixation of CO_2 is inhibited with iodoacetamide, and the CO_2 can be fully recovered in the medium if the inhibited cell is darkened (Fig. 4). If CO_2 assimilation is not inhibited, the rate of transport is at least 100 times the initial rate of photosynthesis (Figs. 3 and 5), and even at steady-state photosynthesis the rate of CO_2 transport is at least three times the rate of photosynthesis. CO_2 uptake clearly precedes O_2 evolution (Fig. 3), and this is consistent with the CO_2 uptake forming the internal pool of inorganic carbon which will support O_2 evolution or photosynthesis (4, 28).

From a large number of experiments, such as that illustrated in Figure 3, the relationship between the transport rate of CO_2 and the substrate concentration was derived (Fig. 5). The $K_{½}$ (CO_2) for CO_2 transport in *Synechococcus* UTEX 625 was 0.4 ± 0.2 μM and maximum rates of transport ranged from 400 to 735 $\mu mol \cdot mg^{-1}$ Chl $\cdot h^{-1}$. These rates of transport were about three times the maximum rates of photosynthesis that were observed with saturating DIC concentrations. One should also note that the initial rate of fluorescence quenching (Fig. 3B), when expressed as a percentage of the maximum rate of change, closely follows the points for CO_2 transport (Fig. 5). The data concerning the initial rate of fluorescence quenching can also be used to calculate a $K_{½}$ (CO_2) for CO_2 transport (Fig. 5, inset), and this value is similar to that determined from the direct measurements of CO_2 transport. The correlation between the initial rate of CO_2 transport and the initial rate of fluorescence quenching was high ($r = 0.98$), as was the correlation between the extent of quenching and the size of the internal inorganic carbon pool ($r = 0.99$) (24). Hence, in cyanobacteria, fluorescence quenching can be used to indirectly estimate initial rates of CO_2 transport and the size of the internal pool. In both cases, quenching seems to be due to the development of the internal carbon pool, but the mechanism of the quenching is not understood.

An earlier report (15) indicated that the K_m (inorganic C) for the transport system in low CO_2-grown *Anabaena* was 141 μM. Subsequently, Volokita *et al.* (31) reported a $K_{½}$ (CO_2) for CO_2 transport of 17 μM, and Badger and Price (7) reported a value of 7 μM for *Synechococcus* PCC 7942. Both of these results were obtained using the silicone fluid centrifugation technique, and although Volokita *et al.* (31) used an exceptionally short sampling time of 5 s, the shortcomings of the technique that we have elaborated still apply. *Anabaena* may well be different from *Synechococcus*, but given that the $K_{½}$ (DIC) for whole cell photosynthesis was 10 μM (0.16 μM CO_2) (15), it is difficult to understand how this could be achieved with inorganic carbon transporters with such low affinity.

The active transport of CO_2 was first demonstrated in 1982 by Badger and Andrews (4) in a marine *Synechococcus*. Since then, active transport or preferential utilization of CO_2 has been shown in a number of cyanobacteria (11, 12, 23, 31). The preferential use of CO_2 has also been demonstrated for a number of green algae (30) and directly measured in *Chlamydomonas* (29). The apparent $K_{½}$ (CO_2) for CO_2 transport in low CO_2-grown *Chlamydomonas* was 0.2 μM, and this was similar to the apparent $K_{½}$ (CO_2) for photosynthesis (29). In low inorganic carbon-grown *Synechococcus*, the $K_{½}$ (CO_2) for photosynthesis was <1.0 μM (6, 16, 17), a concentration similar to the concentration of the $K_{½}$ (CO_2) of the CO_2 transporter reported here. Below the maximum rate of photosynthesis, the rate of photosynthesis is determined by the availability of CO_2 at the site of fixation (16). The delivery of CO_2 to this site in cyanobacteria and microalgae will ultimately depend upon the capacity and the affinity of the transport systems for inorganic carbon, and hence under inorganic carbon limitation, the affinity and capacity of the transport systems will limit the rate of photosynthesis (16). It has been shown that the rate of photosynthesis and the rate of transport as a function of [DIC] are highly correlated (16). Because [CO_2] is normally maintained in the reaction medium at levels approaching zero, the affinity of the CO_2 transporter must be equal to or less than the [CO_2] that would be in equilibrium with the [DIC] that is determining the rate of photosynthesis. Hence, although direct measurements of the affinity of the transport system for CO_2 are essential, at pH 8.0 (at which most is known about the transport system), the $K_{½}$ (CO_2) for photosynthesis may give an indication of the $K_{½}$ of the CO_2 transport system.

Inhibition of CO_2 Transport

Volokita *et al.* (31) presented results showing competition between CO_2 uptake and HCO_3^- uptake in *Anabaena*. On the basis of these results, they proposed that there was only a HCO_3^- transporter and that CO_2 transport occurred via its conversion to HCO_3^- by a front-end CA-like moiety. Competition between CO_2 and HCO_3^- for uptake is also predicted in the DIC transport model proposed by Price and Badger (25) for *Synechococcus* PCC 7942. In this scheme CO_2 from the medium and CO_2 generated from HCO_3^- dehydration within the membrane by an associated front-end mechanism both provide substrate for the CO_2 transport system, which facilitates passage across the membrane along a common path. The contribution of each source to the supply of CO_2 for uptake will depend on the concentration of substrates and the kinetic parameters of the systems (7). In our experiments with *Synechococcus* UTEX 625, we were not able to demonstrate any significant inhibition of CO_2 uptake by HCO_3^- over a range of [$H^{13}CO_3^-$] and transport rates (Figs. 6 and 7). We conclude that the Na^+-dependent mechanism for DIC uptake cannot be a significant source of CO_2 for the CO_2 transport system. Rather, the results suggest that CO_2 transport and Na^+-dependent HCO_3^- transport are separate processes, consistent with previous results (14, 18, 22).

Very high concentrations of HCO_3^- inhibit CO_2 uptake at most about 6% (Fig. 7). Even this inhibition is probably not due to HCO_3^- transport but rather is due to the increasing amounts of $^{13}CO_2$ that would accompany the increasing amounts of $H^{13}CO_3^-$.

That $^{12}CO_2$ can inhibit $^{13}CO_2$ transport is clearly shown in Figures 8 and 9. Without the addition of $^{12}CO_2$, any $^{13}CO_2$ that leaks from the cells or is produced from the dehydration of $H^{13}CO_3^-$ is transported into the cells by the efficient CO_2 pump. When $^{12}CO_2$ is added to the reaction mixture, the $^{13}CO_2$ from the above sources appears in the medium both in the absence of HCO_3^- transport (Fig. 8) or in the presence of HCO_3^- transport (Fig. 9). As expected, for competitive inhi-

bition, increasing amounts of $^{12}CO_2$ cause increasing amounts of $^{13}CO_2$ to appear in the reaction medium.

Within the limited number of cyanobacteria examined in detail, active CO_2 transport would appear to be constitutive because it is present in both high DIC (CO_2) grown cells (2, 5, 19, 25) and low DIC (CO_2) grown cells (2, 5, 10, 20, 25). The CO_2 transport system not only functions in the initial transport of CO_2 into the internal pool but also acts as an effective scavenger of any CO_2 that leaks from the cells during active transport of inorganic carbon. This is quite clearly demonstrated when the CO_2 transport system is inhibited with another isotopic species of CO_2 (Figs. 8 and 9) or with carbonyl sulfide (22) or H_2S (14). Because high levels of CO_2 must exist in the cells for maximum activity of Rubisco, there must be some method available to prevent its rapid dispersion back into the surrounding liquid. Potential barriers that have been suggested are a low conductivity of the cell membrane (3, 5) or a low conductivity of the carboxysome shell (27) or Rubisco itself if CO_2 is generated in the interior of the carboxysome (27). Additionally, conversion of recently transported CO_2 to HCO_3^- by the transport system (25, 31) or by other means would assist in reducing leakage. However, some loss of CO_2 from the cells is inevitable. It would seem that a prominent and effective barrier to prevent this CO_2 from leaking away from the cell is the CO_2 transport system, because its inhibition by various means (Figs. 8 and 9) causes immediate (within 3 s, the response time of the mass spectrometer) and substantial leakage of CO_2 from the cells to the environment.

Because the substrate for Rubisco is CO_2, high rates of carbon assimilation would always require high levels of CO_2 in the vicinity of the enzyme. For an effective system, the potential diffusion of CO_2 away from this site (*i.e.* leakage) must be prevented. Hence, it would seem that all organisms, whether cyanobacteria or algae, that concentrate inorganic carbon must possess a CO_2 transport system in addition to the other leak control mechanisms to fill this role. To be maximally effective, the affinity of the transporter, as demonstrated here, must be very high. Only with such a system for active CO_2 transport would the cells be able to maximize their ability to compete for limiting DIC and to utilize all of the available DIC from the medium.

LITERATURE CITED

1. **Abe T, Tsuzuki M, Miyachi S** (1987) Transport and fixation of inorganic carbon during photosynthesis of *Anabaena* grown under ordinary air. I. Active species of inorganic carbon utilized for photosynthesis. Plant Cell Physiol **28:** 273–281
2. **Abe T, Tsuzuki M, Miyachi S** (1987) Transport and fixation of inorganic carbon during photosynthesis in cells of *Anabaena* grown under ordinary air. III. Some characteristics of the HCO_3^- transport system in cells grown under ordinary air. Plant Cell Physiol **28:** 867–874
3. **Badger MR** (1987) The CO_2-concentrating mechanism in aquatic phototrophs *In* MD Hatch, NK Boardman, eds, The Biochemistry of Plants: A Comprehensive Treatise, Vol 10. Academic Press, New York, pp 219–274
4. **Badger MR, Andrews TJ** (1982) Photosynthesis and inorganic carbon usage by the marine cyanobacterium *Synechococcus* sp. Plant Physiol **70:** 517–523
5. **Badger MR, Bassett M, Comins HN** (1985) A model for HCO^-_3 accumulation and photosynthesis in the cyanobacterium *Synechococcus* sp. Plant Physiol **77:** 465–471
6. **Badger MR, Gallagher A** (1987) Adaptation of photosynthetic CO_2 and HCO_3^- accumulation by the cyanobacterium *Synechococcus* PCC 6301 to growth at different inorganic carbon concentrations. Aust J Plant Physiol **14:** 189–201
7. **Badger MR, Price GD** (1990) Carbon oxysulfide is an inhibitor of both CO_2 and HCO_3^- uptake in the cyanobacterium *Synechococcus* PCC 7942. Plant Physiol **94:** 35–39
8. **Buch K** (1960) Dissoziation der Kohlensäure, Gleichgewichte und Puffer systeme *In* W Ruhland, ed, Handbuch der Pflanzenphysiologie, Vol 1. Springer Verlag, Berlin, pp 1–11
9. **Colman B, Espie GS** (1985) CO_2 uptake and transport in leaf mersophyll cells. Plant Cell Environ **8:** 449–457
10. **Espie GS, Canvin DT** (1987) Evidence of Na^+-independent HCO_3^- uptake by the cyanobacterium *Synechococcus leopoliensis*. Plant Physiol **84:** 125–130
11. **Espie GS, Gehl KA, Owttrim GW, Colman B** (1984) Inorganic carbon utilization by cyanobacteria. *In* C Sybesma, ed, Advances in Photosynthesis Research, Proceedings of the International Congress on Photosynthesis, Brussels, Belgium, Vol 3. Martinus Nijoff/Dr W Junk Publishers, The Hague, pp 457–460
12. **Espie GS, Miller AG, Birch DG, Canvin DT** (1988) Simultaneous transport of CO_2 and HCO^-_3 by the cyanobacterium *Synechococcus* UTEX 625. Plant Physiol **87:** 551–554
13. **Espie GS, Miller AG, Canvin DT** (1988) Characterization of the Na^+-requirement in cyanobacterial photosynthesis. Plant Physiol **88:** 757–763
14. **Espie GS, Miller AG, Canvin DT** (1989) The selective and reversible inhibition of active CO_2 transport by hydrogen sulfide in a cyanobacterium. Plant Physiol **91:** 387–394
15. **Kaplan A, Badger MR, Berry JA** (1980) Photosynthesis and the intracellular inorganic carbon pool in the blue-green alga *Anabaena variabilis*: response to external CO_2 concentration. Planta **149:** 219–226
16. **Mayo WP, Elrifi IR, Turpin DH** (1989) The relationship between ribulose bisphosphate concentration, dissolved inorganic carbon (DIC) transport and DIC-limited photosynthesis in the cyanobacterium *Synechococcus leopoliensis* grown at different concentrations of inorganic carbon. Plant Physiol **90:** 720–727
17. **Mayo WP, Williams TG, Birch DG, Turpin DH** (1986) Photosynthetic adaptation by *Synechococcus leopoliensis* in response to exogenous dissolved inorganic carbon. Plant Physiol **80:** 1038–1040
18. **Miller AG, Canvin DT** (1985) Distinction between HCO^-_3 and CO_2 dependent photosynthesis in the cyanobacterium *Synechococcus leopoliensis* based on the selective response of HCO^-_3 transport to Na^+. FEBS Lett **187:** 29–32
19. **Miller AG, Canvin DT** (1987) Na^+-stimulation of photosynthesis in the cyanobacterium *Synechococcus* UTEX 625 grown on high levels of inorganic carbon. Plant Physiol **84:** 118–124
20. **Miller AG, Espie GS, Canvin DT** (1988) Active transport of CO_2 by the cyanobacterium *Synechococcus* UTEX 625. Measurement by mass spectrometry. Plant Physiol **86:** 677–683
21. **Miller AG, Espie GS, Canvin DT** (1988) Chlorophyll *a* fluorescence yield as a monitor of both active CO_2 and HCO^-_3 transport by the cyanobacterium *Synechococcus* UTEX 625. Plant Physiol **86:** 655–658
22. **Miller AG, Espie GS, Canvin DT** (1989) The use of COS, a structural analog of CO_2, to study active CO_2 transport in the cyanobacterium *Synechococcus* UTEX 625. Plant Physiol **90:** 1221–1231
23. **Miller AG, Espie GS, Canvin DT** (1990) Physiological aspects of CO_2 and HCO_3^- transport by cyanobacteria: a review. Can J Bot **68:** 1291–1302

24. **Miller AG, Espie GS, Canvin DT** (1991) The effects of inorganic carbon and oxygen upon fluorescence in the cyanobacterium *Synechococcus* UTEX 625. Can J Bot **69:** 1151–1160
25. **Price GD, Badger MR** (1989) Ethoxyzolamide inhibition of CO_2 uptake in the cyanobacterium *Synechococcus* PCC7942 without apparent inhibition of internal carbonic anhydrase activity Plant Physiol **89:** 37–43
26. **Price GD, Badger MR** (1989) Ethoxyzolamide inhibition of CO_2-dependent photosynthesis in the cyanobacterium *Synechococcus* PCC7942 Plant Physiol **89:** 44–50
27. **Reinhold L, Zviman M, Kaplan A** (1989) A quantitative model for inorganic carbon fluxes and photosynthesis in cyanobacteria. Plant Physiol Biochem **27:** 945–954
28. **Shelp BJ, Canvin DT** (1984) Evidence for bicarbonate accumulation by *Anacystis nidulans*. Can J Bot **62:** 1398–1403
29. **Sültemeyer DF, Fock HP, Canvin DT** (1991) Active uptake of inorganic carbon by *Chlamydomonas reinhardtii*. Evidence for simultaneous transport of HCO_3^- and CO_2 and characterization of active CO_2 transport. Can J Bot **69:** 995–1002
30. **Tsuzuki M, Miyachi S** (1989) The functions of carbonic anhydrase in aquatic photosynthesis. Aquatic Bot **34:** 85–104
31. **Volokita M, Zenvirth D, Kaplan A, Reinhold L** (1984) Nature of the inorganic carbon species actively taken up by the cyanobacterium *Anabaena variabilis*. Plant Physiol **76:** 599–602